The Journal of Physical Chemistry Letters

Letter

pubs.acs.org/JPCL

Bile Acid Binding Protein Functionalization Leads to a Fully Synthetic Rhodopsin Mimic

Katiuscia Pagano,[†,∥] Marco Paolino,[*,‡,∥] Stefania Fusi,[‡] Vinicio Zanirato,[§] Claudio Trapella,[⊥] Germano Giuliani,[‡] Andrea Cappelli,[‡] Serena Zanzoni,[¶] Henriette Molinari,[†] Laura Ragona,[*,†] and Massimo Olivucci[*,‡,#]

[†]Istituto per lo Studio delle Macromolecole, CNR, Via A. Corti 12, 20133 Milano, Italy

[‡]Dipartimento di Biotecnologie, Chimica e Farmacia (Dipartimento di Eccellenza 2018-2022), Università degli Studi di Siena, Via Aldo Moro 2, 53100 Siena, Italy

[§]Dipartimento di Scienze Chimiche e Farmaceutiche and [⊥]Laboratory for Technologies of Advanced Therapies (LTTA), Department of Chemical and Pharmaceutical Sciences, Università di Ferrara, 44121 Ferrara, Italy

[¶]Centro Piattaforme Tecnologiche, Università di Verona, Strada Le Grazie, 37134 Verona, Italy

[#]Chemistry Department, Bowling Green State University, Bowling Green, Ohio 43403, United States

Supporting Information

ABSTRACT: Rhodopsins are photoreceptive proteins using light to drive a plethora of biological functions such as vision, proton and ion pumping, cation and anion channeling, and gene and enzyme regulation. Here we combine organic synthesis, NMR structural studies, and photochemical characterization to show that it is possible to prepare a fully synthetic mimic of rhodopsin photoreceptors. More specifically, we conjugate a bile acid binding protein with a synthetic mimic of the rhodopsin protonated Schiff base chromophore to achieve a covalent complex featuring an unnatural protein host, photoswitch, and photoswitch-protein linkage with a reverse orientation. We show that, in spite of its molecular-level diversity, light irradiation of the prepared mimic fuels a photochromic cycle driven by sequential photochemical and thermal Z/E isomerizations reminiscent of the photocycles of microbial rhodopsins.

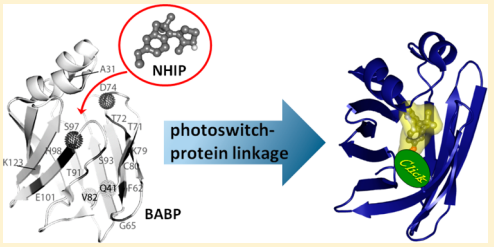

Molecular photoswitches are a class of molecules capable of alternating between at least two distinct equilibrium forms via light irradiation[1−7] with promising application in material science, biological science, and photopharmacology.[8−11] Photoswitches are also largely used by nature for triggering a plethora of different functions initiated with the transformation of light energy into protein structure modifications, which, in turn, drive complex biological functions.[12] Among natural systems, rhodopsins[13] constitute an ecologically widespread class of membrane photoresponsive proteins driving fundamental functions through the action of a natural photoswitch, namely the protonated Schiff base of retinal (rPSB).[14−16] rPSB triggers the rhodopsin photocycles by undergoing a unidirectional and regioselective clockwise or counterclockwise double-bond photoisomerization and, ultimately, activating functions such as vision, pupillary reflexes, chromatic adaptation, ion-gating, and ion pumping.[17−21] In spite of their different functions, rhodopsins are characterized by a remarkably common architecture featuring seven α-helices forming a cavity hosting rPSB chromophore covalently bound to a lysine residue located in the protein cavity. Furthermore, the functions of the protein are always initiated by the photoisomerization of rPSB. The fact that the functionality of rhodopsins can be modulated by variations in the amino acid sequence appears to be important for the design of protein-based molecular devices. With such target in mind, it is hoped that the development of a fully synthetic rhodopsin mimic can provide the necessary prototype system.

In recent years, rhodopsin mimics have been developed using intracellular lipid binding protein (iLBP), such as CRABPII, as scaffolds capable of binding all-*trans* rPSB.[22−26] The engineered protein/retinal covalent constructs could be useful as research tools useful for understanding the mechanisms of light exploitation at the molecular level. The target was to use such easy to engineer and crystallize systems to study, through a bottom-up approach, fundamental aspects of protein−rPSB interactions and reveal how photoswitching could be effectively implemented in nature.[13,27] However, in spite of their interest for mechanistic studies, the reported rhodopsin mimics are semisynthetic as they incorporate the natural photoswitch. Thus, they do not offer the variability of a synthetic construct where both the protein and the Schiff base photoswitch are unnatural. To the best of our knowledge, such fully synthetic rhodopsin mimics have not been reported.

Received: January 23, 2019
Accepted: April 15, 2019
Published: April 15, 2019

DOI: 10.1021/acs.jpclett.9b00210
J. Phys. Chem. Lett. XXXX, XXX, XXX−XXX

In the past, we have carried out extensive work[27−30] on the design, synthesis, and characterization of unnatural photoswitches capable of mimicking the photophysics of bovine rhodopsin (Rh),[31] a widely studied dim-light visual pigment. These fully organic compounds were based on *N*-alkylated or N-protonated indanylidene pyrroline Schiff bases (NAIP or NHIP, respectively) in which the indene moiety, representing the stator, and the pyrroline portion, working as a rotor, are connected by an isomerizable double bond.[32−35] In fact, NAIP and NHIP perform a regioselective subpicosecond double bond photoisomerization comparable to that observed for the 11-*cis* rPSB chromophore embedded in the Rh pocket.[36] Moreover, NAIP and NHIP derivatives undergo, in solution, an ultrafast photoisomerization with a 20% quantum yield and displaying low-frequency (60 to 80 cm^{-1}, i.e., ∼500 fs period) oscillatory features similar to those observed in visual pigments and light-sensing pigments featuring a 11-*cis* or 13-*cis* rPSB chromophore, respectively.[29] Furthermore, NAIPs and NHIPs represent prototypes of light-driven single-molecule molecular rotors of the Feringa's type.[7,37,38] In fact, they share with such hydrocarbon rotors a skeleton with a single exocyclic isomerizable double bond, but, due to their cationic nature and protonated imine moiety, they mimic the functional group of the retinal chromophore. The photochemical properties of NAIPs and NHIPs can be compared with those of the Feringa's type rotors,[7,38] which, however, display excited state lifetimes ranking from 0.2 to 3 ps and a quantum yield typically below 2% without showing coherent vibrational oscillations.[37]

Here, we design, prepare, and characterize a first, fully synthetic rhodopsin mimic. To achieve this result we decided to combine an unnatural N-protonated indanylidene pyrroline Schiff bases (NHIP)[32−35] photoswitch, capable to mimic the photochemical behavior of the rPSB, with a bile acid binding protein (BABP). BABP has been selected as our reference framework for three different reasons. First, BABP and CRABPII belongs to the same intracellular lipid binding protein (iLBP) family[39] with sequences sharing 31% identity and 47% similarities and resulting in a structural alignment displaying a RMSD of 1.6 Å. This indicates that, like CRABPII, BABP could be employed in the engineering of rhodopsin mimics. This conclusion is further supported by BABP structural stability to mutagenesis, its dynamics, allowing promiscuous ligand binding[40] and, finally, its high expression levels resulting in the production of high protein quantities (>90 mg × L^{-1}).[41] Second, in the past some of us have investigated the interactions of BABP cavity (defined by a *β*-barrel fold) and several ligands.[40,42−45] Such background appears to be instrumental in determining whether the BABP cavity could be suitably functionalized to build biomimetic host−guest complexes. Third, BABP was shown to bind bile salts with a 1:2 stoichiometry and accommodate two bile salts in two distinct sites (generally defined as Site 1 and Site 2) of the internal cavity with high affinity.[46] Thanks to this peculiarity, the photoisomerization of NHIP, which fully occupies Site 2 in the presented construct, could alter the affinity for the bile salt hosted in Site 1, potentially generating a photoresponsive delivery system to be constructed/investigated in the future. The above reasons indicate that BABP-based fully synthetic rhodopsin mimics could be prepared by following the general strategy employed for CRABPII based semisynthetic constructs. Accordingly, our effort starts with NMR and experimentally driven docking studies of the noncovalent complex formed by incorporation of the rigid NAIP framework into the BABP *β*-barrel fold defining a binding cavity. As detailed further, after showing that the photoswitch can penetrate the protein cavity, we demonstrate that the orthogonal addition of a cysteine SH group, located at the bottom of the BABP pocket, with the propargyl maleimide double-bond, provides a monopropargylated protein capable to covalently link a tailored NHIP photoswitch bearing a tail terminating with an azido group. Finally, by employing extensive NMR analysis, we show that the obtained mimic displays a type-T photochromism (i.e., where the E → Z stereoisomer conversion is light-driven and the Z → E back conversion is thermally driven).[47]

CAVITY PENETRATION

The *N*-alkylated indanylidene pyrroline Schiff bases (**MeO-NAIP**) photoswitch of Scheme 1 was titrated into different

Scheme 1. Structure of MeO-NAIP and MeO-NHIP Photoswitches Employed for Investigation of Noncovalent Host−Guest Complexes with BABP[a]

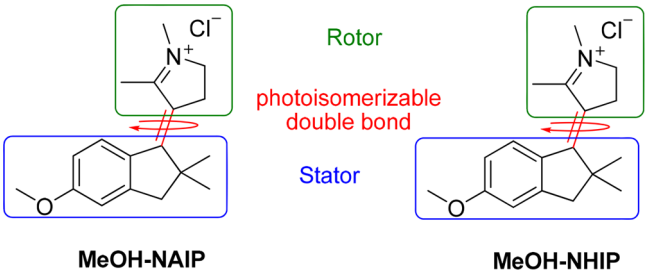

[a]In both cases, we only display the Z-stereoisomer.

BABP isoforms, ^{15}N-BABP or ^{15}N-BABP/SS[48] (with and without a free thiol group), and a series of ^{1}H−^{15}N-heteronuclear single quantum coherence (HSQC) NMR spectra were recorded. These experiments are widely employed in protein−ligand interaction studies because chemical shifts are indicators of binding events or conformational rearrangements. HSQC spectra recorded for both ^{15}N-BABP and ^{15}N-BABP/SS in the absence and presence of **MeO-NAIP** at different protein/Schiff base ratios, together with the weighted average of ^{1}H and ^{15}N chemical shift perturbation (CSP) and changes observed in peak intensity upon **MeO-NAIP** addition are reported in Figure S1. For both proteins, the titration progress displays binding events occurring on fast exchange on the NMR time scale with a distribution of residues affected by the binding similar to that obtained with the putative ligands (bile acids).[49,50] These results show that **MeO-NAIP** enters into the protein pocket (a K_d in the mM range was estimated on the basis of CSPs, see Figure S2).

The less sterically hindered **MeO-NHIP** (Scheme 1), lacking the methyl group on the nitrogen atom,[51] was also tested. The analysis of the weighted average of ^{1}H and ^{15}N CSP and of the intensity changes indicated that BABP/SS residues involved in the interaction with **MeO-NHIP** are the same observed for **MeO-NAIP** (Figures 1A−D and S3) and that the switch is internalized in the protein *β*-barrel. Data fitting carried out using eq 1 in the Supporting Information, suggested a slightly improved affinity (K_d in the range 700−900 *μ*M) for the N-protonated photoswitch with respect to the *N*-methylated one.

DOI: 10.1021/acs.jpclett.9b00210
J. Phys. Chem. Lett. XXXX, XXX, XXX−XXX

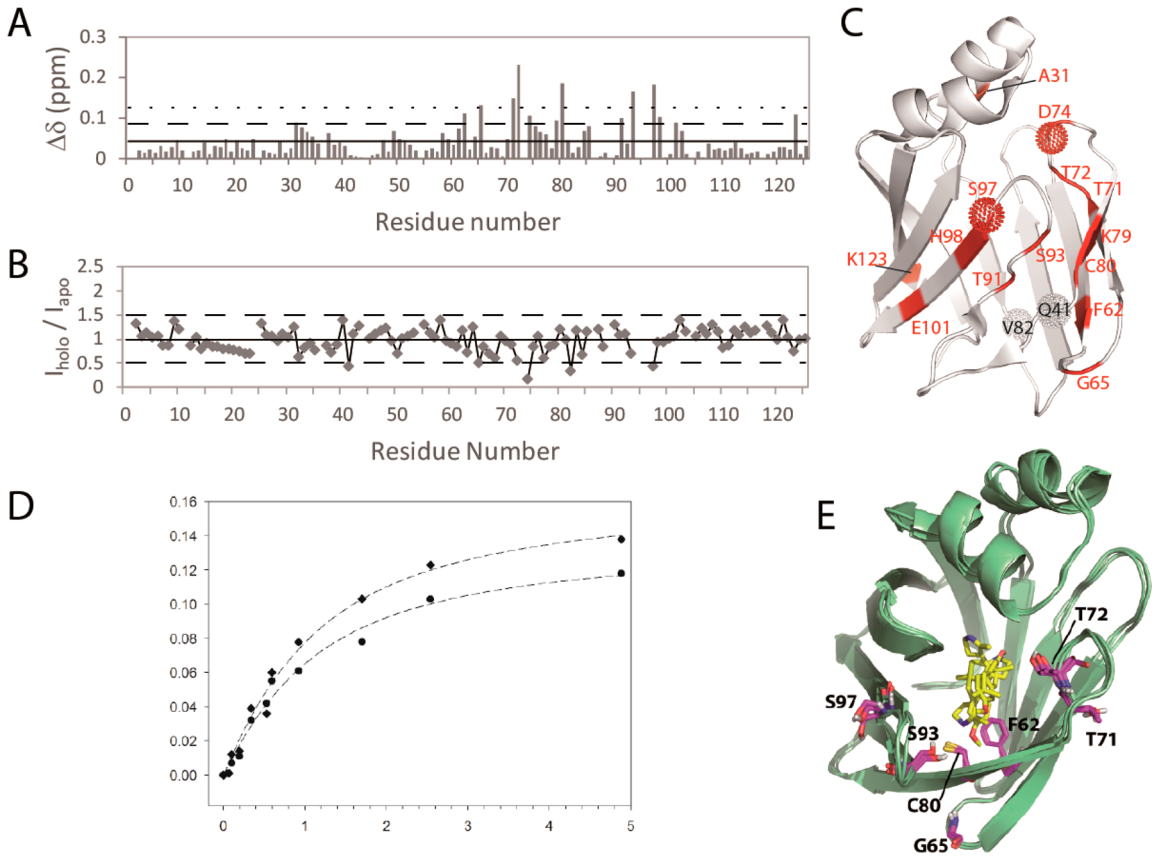

Figure 1. (A) Graphical representation of the combined H^N and ^{15}N CSP upon **MeO-NHIP** addition at a protein/MeO-NHIP 1:7.5 molar ratio, as observed for BABP/SS at pH 5.5. CSP average value (⟨CSP⟩), ⟨CSP⟩ + 1σ, and ⟨CSP⟩ + 2σ values are indicated as straight, dashed, and dotted lines, respectively. (B) $^1H-^{15}N$ HSQC cross peaks intensities ratio profiles (defined as normalized holo cross-peak volume/apo cross-peak volume) upon **MeO-NHIP** addition to BABP-SS. The horizontal dashed lines mark intensity changes higher/lower than 50% (C) BABP/SS residues showing CSP higher than (⟨CSP⟩ + 1σ) upon **MeO-NHIP** addition are highlighted in red on the structure. Residues showing significant intensity decrease (>50%) upon **MeO-NHIP** addition are highlighted as dotted spheres. (D) Chemical shift perturbation of ^1H frequencies of residues T72 (circle) and C80 (diamond) as a function of **MeO-NHIP** concentration, as derived from a titration experiment of a protein sample 0.65 mM. Data fitting is represented using a dashed line. (E) Superposition of the first structures of the best three clusters obtained with HADDOCK. BABP-SS is shown as a green cartoon, **MeO-NHIP** is shown in yellow sticks. F62, G65, T71, T72, C80, S93, S97, set as active residues in docking calculation, are shown as purple sticks.

To test whether **MeO-NHIP** is buried inside the protein and investigate its preferred orientations, a structural model of the complex **BABP/SS-MeO-NHIP** has been built employing the data driven HADDOCK docking software.[52,53] The best solutions confirmed that **MeO-NHIP** is completely embedded in the BABP-SS β-barrel, exhibiting different poses (Figure 1E).

FUNCTIONALIZATION OF BABP CAVITY

In spite of its low value, the photoswitch binding affinity observed in noncovalent BABP/**MeO-NHIP** complexes point to a stability large enough to allow for a conjugation reaction. Because of their lower frequency in natural proteins, SH groups of cysteine residues were targeted for conjugation as they are effective reactants in thiolo-ene click chemistry.[54−56] BABP has a single cysteine residue (C80), located at the bottom of the β-barrel with its SH group exposed in the protein pocket, and it is an ideal candidate for conjugation. As summarized in Scheme 2, a combination of two click chemistry couplings was chosen to prepare a covalent complex with chemical selectivity. First, a propargyl group anchored to maleimide was introduced in BABP by thiolo-ene coupling. Subsequently, well-known copper catalyzed Azido-Alkyne click reaction was optimized to conjugate an azido functionalized NHIP derivative (**^{13C}NHIP-N$_3$**).[57]

The N-propargyl-maleimide reagent was selected to functionalize the cysteine residue with the required alkyne moiety. The reaction conditions were optimized using unsubstituted maleimide, the same reaction conditions were successfully employed for the functionalization of unlabeled (U) and ^{15}N labeled BABPs (enriched 90−95% in ^{15}N) with *N*-propargyl-maleimide, yielding **U-BABP-Prop** and **^{15}N-BABP-Prop**. Reaction completion was checked by mass spectrometry (Figure S4) and protein correct fold by NMR (Figure S5).

To covalently combine the photoswitch inside the protein pocket, through a CuAAC (1,3-dipolar copper(I)-catalyzed azide−alkyne cycloaddition) reaction (Scheme 2),[58,59] we noticed that the previously discussed HADDOCK structures (Figure 1) showed favored solutions with the **MeO-NHIP** methoxy group located in the proximity of the C80 thiol group. Thus, the methoxy group of **MeO-NHIP** was replaced by an azido terminated ethoxy chain. The compounds **NHIP-N$_3$** and its labeled analogue **^{13}C-NHIP-N$_3$** were prepared as detailed in the SI and summarized in Scheme S1. The noncovalent binding of such derivative was verified by NMR exploiting the

DOI: 10.1021/acs.jpclett.9b00210
J. Phys. Chem. Lett. XXXX, XXX, XXX−XXX

Scheme 2. Synthesis of Conjugated Labeled (^{15}N) or Unlabeled (U-) BABPs Proteins with NHIP Isotopomers

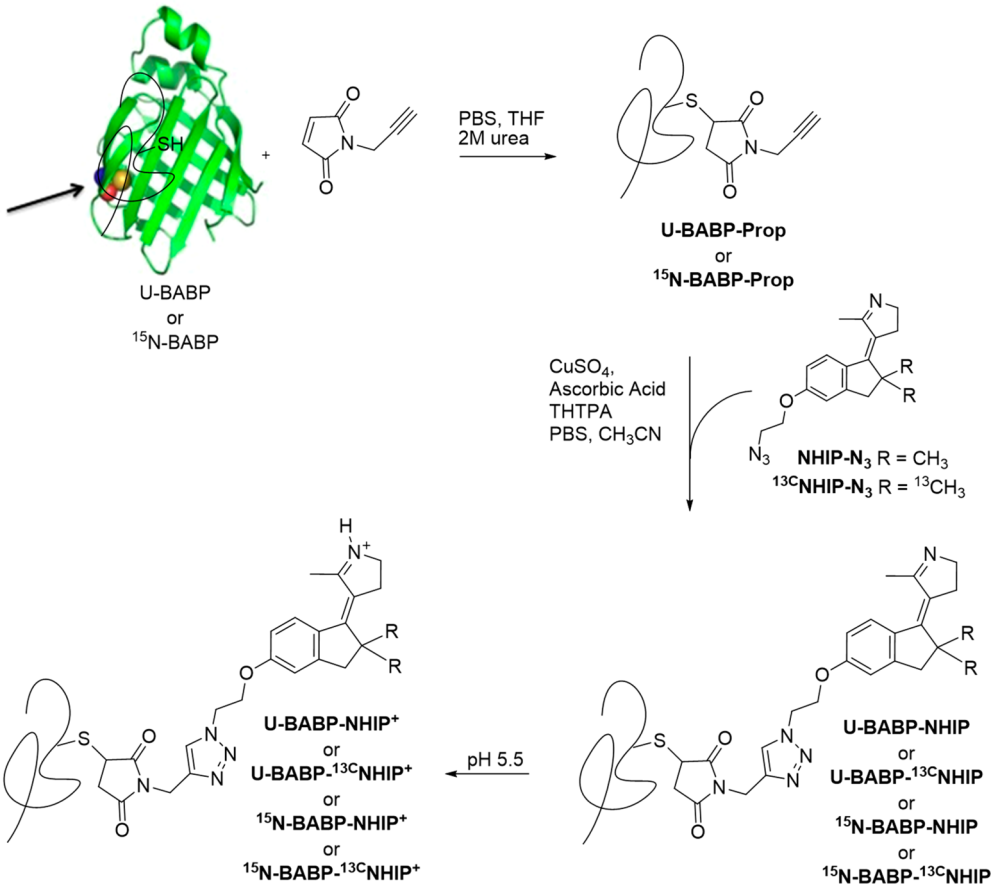

presence of ^{13}C labeled methyl groups on **^{13C}NHIP-N$_3$** (Figure S6).

NHIP-N$_3$ and its labeled analogue **^{13}C-NHIP-N$_3$** were employed for CuAAC reaction with both **U-BABP-Prop** and **^{15}N-BABP-Prop**. Although CuAAC has been described as an excellent method for bioconjugation,[60−62] many precautions had to be taken to obtain an exhaustive monoderivatization of the proteins, avoiding oxidative degradation[60] and protein unfolding (see reaction conditions in the Supporting Information).[63] The mass spectra of the final **BABP-NHIP** functionalized protein are displayed in Figure S7. The **^{15}N-BABP-^{13C}NHIP** sample was analyzed by NMR, exploiting nitrogen and carbon labeling to observe the protein and the bound photoswitch (Figure S8). The increase of the protein line width is indicative of conformational exchange, in line with the coexistence of different conformations of the NHIP chain in the pocket possibly affecting backbone flexibility (*vide infra*). NHIP localization within the protein cavity was further investigated by binding experiments performed treating **U-BABP-^{13C}NHIP** with sodium glycochenodeoxycholate (GCDA), the protein putative ligand. BABP was indeed shown to bind bile salts with a 1:2 stoichiometry, simultaneously accommodating two bile salts in its internal cavity with high affinity, thus forming a ternary complex. The addition to unlabeled BABP of ^{15}N-labeled glycochenodeoxycholic acid (GCDA), monitored by heteronuclear ^{1}H−^{15}N HSQC, revealed three distinct sets of signals, corresponding to ligand in the unbound form, and bound to the two binding sites, Site 1 and Site 2, characterized by different chemical environments.[46] Titration of **U-BABP-^{13C}NHIP** with ^{15}N-GCDA showed that the protein could still bind GCDA in the more superficial Site 1,[50,64] while the bound photoswitch prevented access to the internal Site 2 (Figure 2). This observation confirms that, upon covalent binding of the photoswitch, the native BABP fold required for GCDA binding is conserved.

SPECTROSCOPIC AND PHOTOCHEMICAL CHARACTERIZATION

The **^{13C}NHIP-N$_3$** chromophore in water solution at pH 7.2 shows an absorption spectrum dominated by a band centered

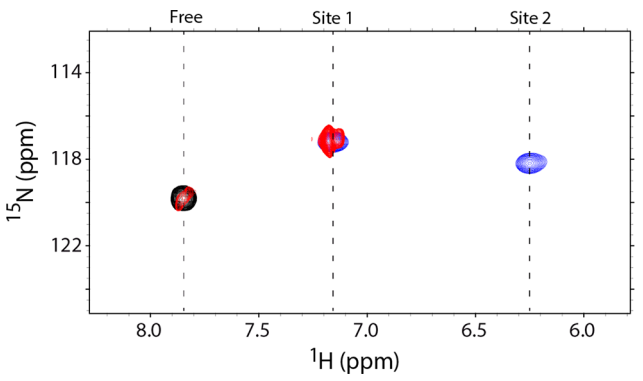

Figure 2. Overlap of ^{1}H−^{15}N HSQC spectra of ^{15}N-GCDA free (black), noncovalently bound to BABP (blue), and to **U-BABP-^{13C}NHIP** (red).

DOI: 10.1021/acs.jpclett.9b00210
J. Phys. Chem. Lett. XXXX, XXX, XXX−XXX

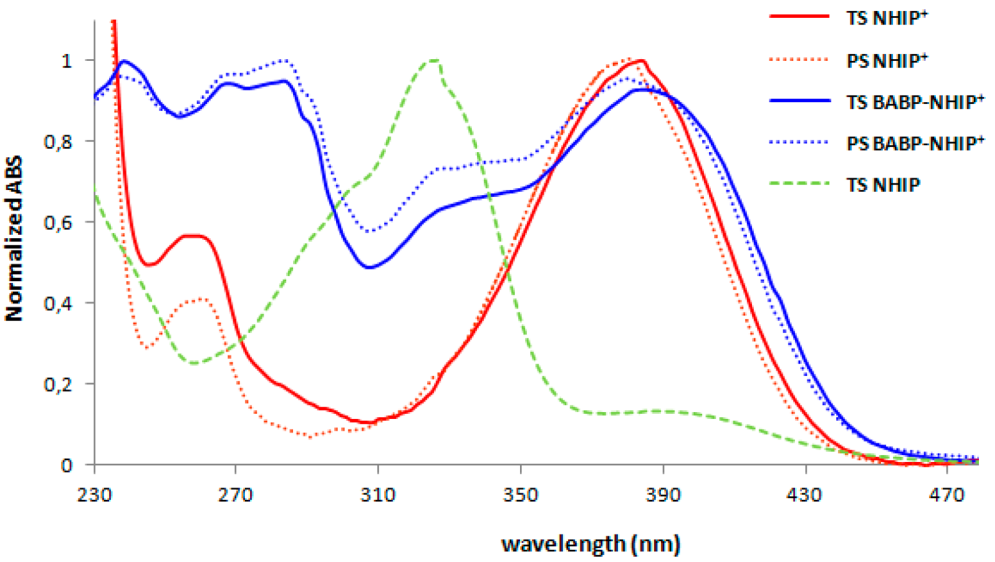

Figure 3. Normalized UV−vis absorption spectra of the thermally equilibrated state (TS) of **NHIP-N_3** registered in water solution at pH 7.2 (dashed green line), and at pH 5.5 (red line), and of its photostationary state (PS) obtained after 16 h irradiation at 400 nm (dotted red line) compared with the normalized UV−vis absorption spectra of the TS of **BABP-NHIP** registered at pH 5.5 (blue line) and of the its PS obtained in the same conditions (dotted blue line).

at about 320 nm (Figure 3). The same chromophore at pH 5.5 shows a maximum at about 380 nm and a tail, which persists up to 450 nm. The observed bathochromic shift can be attributed to the complete protonation of the imine nitrogen at pH 5.5, as previously reported for the **MeO-NAIP** and **MeO-NHIP**.[33] The absorption spectrum of **^{15}N-BABP-^{13C}NHIP** at pH 5.5 shows, in addition to a structured ultraviolet region attributable to the protein, the presence of a broader absorption centered at about 382 nm for the most part overlapping with the absorption spectrum of **MeO-NHIP**. In the dark (i.e., thermally equilibrated) state both **^{13C}NHIP-N_3** and **^{15}N-BABP-^{13C}NHIP** at pH 5.5 exhibited a predominance of E-stereoisomer population (90 and 83%, respectively), as estimated from NMR methyl resonances volumes. The 7% increase in the *Z*-stereoisomer in **^{5}N-BABP-^{13C}NHIP** is likely to reflect a decrease in unfavorable interaction between the protein cavity and the less populated stereoisomer.

Irradiation of **^{13C}NHIP-N_3** and **^{15}N-BABP-^{13C}NHIP** in solution at pH 5.5, where the NHIP imine head is protonated (i.e., to mimic the rPSB chromophore of rhodopsins), at 400 nm for 16 h leads to a photostationary state displaying, in both cases, a slight blue-shift of the 380 nm absorption attributable to an increase in the Z-stereoisomer.[33] The prolonged irradiation, (i) guarantees reaching the NHIP photostationary state, (ii) allows the protein to conformationally relax after NHIP isomerization and (iii) allows testing the photochemical stability of the **NHIP-N_3** and **N-BABP-NHIP**. After switching off light irradiation, the thermal relaxations of the isolated and BABP-linked photoswitch were investigated by NMR thanks to the distinct chemical shifts of the E and Z isomers. This technique offers the possibility of exploiting different labeling schemes for the protein (nitrogen labeling) and the ligand (carbon labeling) to observe simultaneously both protein and bound photoswitch. Moreover, NMR studies give the opportunity to verify that the structural changes occurring at the photoswitch level after irradiation do not affect the protein folding. Therefore, a series of ^{1}H−^{13}C HSQC spectra were recorded over time and the cross peak volume of the methyl resonances of the two stereoisomers were plotted as a function of time (Figure 4A,C). The results (Figure 4B,D) indicate very different kinetics for the thermal relaxation of the free and bound species. This difference is interpreted in terms of Z → E thermal isomerization leading to a completely restored thermal Z/E equilibrium after ∼ 2.5 h for the free compound. At variance, in **^{15}N-BABP-^{13C}NHIP**, the isomeric equilibrium was not restored even after 5 h. Interestingly, ^{1}H−^{15}N HSQC spectra of the protein confirmed that changes occurring at the photoswitch during and after irradiation did not affect the global fold of the protein.

The fitting of the experimental data allowed us to estimate/extrapolate the E/Z composition of the photostationary states, not directly determinable by ^{1}H−^{13}C HSQC, due to the time required for spectra acquisition. Interestingly, **^{13C}NHIP-N_3** bound to the protein showed 66 ± 3% of Z stereoisomer in the photostationary state, a value similar to the 72 ± 3% value calculated in the same conditions for the free photoswitch and in line with that previously reported for the related **MeO-NAIP** in methanol solution. This behavior suggests that the protein environment does not limit the efficiency of the E → Z photoisomerization. However, the significant delay of the return to the equilibrium observed for BABP-bounded NHIP with respect to NHIP in solution (see above), indicates that the photoswitch-protein interactions increase the energy barrier controlling the Z → E thermal isomerization, thus "trapping" the NHIP Z stereoisomer.

In conclusion, above we have reported on the covalent binding a NHIP protonated Schiff basis photoswitch to BABP. As shown by extensive NMR studies, BABP provides a suitable environment for hosting NHIP derivatives. Furthermore, enough experimental evidence has been collected, which indicates that a fully synthetic rhodopsin mimic has been achieved. Indeed, our **BABP-NHIP** features four characteristics consistent with our synthetic and NMR studies: (i) an unnatural protonated Schiff base photoswitch, qualitatively different from the natural rPSB of rhodopsins, covalently linked inside the BABP pocket, (ii) an unnatural photoswitch-protein linkage, chemically different from the imine linkage of rhodopsins, but obtained in conditions preserving the native

DOI: 10.1021/acs.jpclett.9b00210
J. Phys. Chem. Lett. XXXX, XXX, XXX−XXX

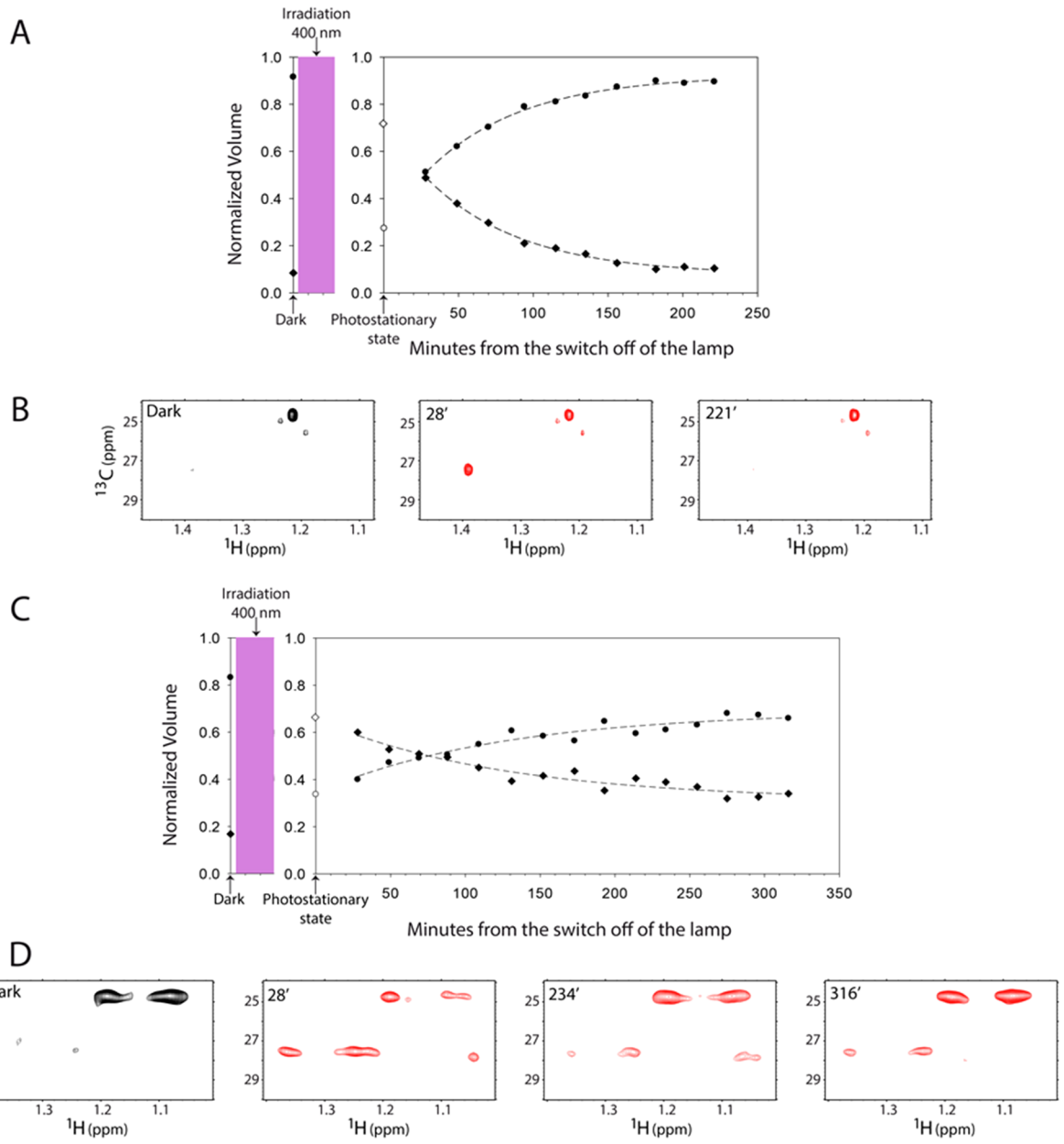

Figure 4. Difference between time evolution of E and Z stereoisomers of free (A) ^{13C}**NHIP-N$_3$** and (C) ^{15}**N-BABP-**^{13C}**NHIP**, after illumination. The normalized cross peak volume of the methyl resonances of the two stereoisomers, as measured in ^{1}H−^{13}C HSQC spectra recorded at variable times after switching off the irradiation, are reported: E and Z stereoisomers are indicated as full circle and diamonds, respectively. The volumes measured before light irradiation are labeled as "Dark", while the estimated populations of the photostationary states are reported as empty circles and diamonds for E and Z stereoisomers, respectively. Panels B and D report selected ^{1}H−^{13}C HSQC spectra of free and covalently bound ^{13C}**NHIP**, respectively, in the dark state and at different elapsed times after switching the irradiation off. Notice that the linkage of the cysteine to N-propargyl-maleimide give rise to two diastereoisomers which, may exhibit multiple conformers, reflected in the heterogeneity observed in the BABP-bounded ^{13C}**NHIP** chromophore.

protein structure, (iii) an unnatural (inverted) orientation of the protonated Schiff base C = NH(+) group, which points toward the cavity exit rather than being located at its bottom and finally (iv) a type-T photochromism similar to the one observed in microbial rhodopsins.[65−67] These results also represent the first applicative example of NAIP/NHIP photoswitchable molecules to the design and construction of a prospective functional molecular device. Excited state dynamics and photoisomerization quantum efficiency of our construct will be investigated by carrying out the same time-resolved studies reported for MeO-NAIP and MeO-NHIP and for microbial rhodopsins to enhance its understanding and future applicability.[29,68] Furthermore, as anticipated above, our BABP-NHIP construct could provide the basis for the development of novel light-triggered delivery systems.

■ ASSOCIATED CONTENT

Ⓢ Supporting Information

The Supporting Information is available free of charge on the ACS Publications website at DOI: 10.1021/acs.jpclett.9b00210.

DOI: 10.1021/acs.jpclett.9b00210
J. Phys. Chem. Lett. XXXX, XXX, XXX−XXX

NMR titration data; chemical shift data; superimposition data; mass spectra; synthesis of photoswitches; reagents formation; materials and methods (PDF)

AUTHOR INFORMATION

Corresponding Authors

*E-mail: paomar@oneonline.it.
*E-mail: laura.ragona@ismac.cnr.it.
*E-mail: olivucci@unisi.it.

ORCID

Marco Paolino: 0000-0003-1387-7875
Andrea Cappelli: 0000-0003-4140-3028
Henriette Molinari: 0000-0002-3678-130X
Laura Ragona: 0000-0003-3893-7117
Massimo Olivucci: 0000-0002-8247-209X

Author Contributions

‖These authors contributed equally.

Notes

The authors declare no competing financial interest.

ACKNOWLEDGMENTS

M.P., S.F., G.G., A.C., and M.O. are grateful for a MIUR (Ministero dell'Istruzione, dell'Università e della Ricerca) grant "Dipartimento di Eccellenza 2018−2022". H.M., K.P., and L.R. gratefully acknowledge Fondazione Antonio De Marco (Italy) for financial support. The financial contribution of MIUR, PRIN 2015 (2015RNWJAM) is also acknowledged. Chiara Botta (ISMAC) is acknowledged for the access to ISMAC Optical Facility.

REFERENCES

(1) Kathan, M.; Hecht, S. Photoswitchable molecules as key ingredients to drive systems away from the global thermodynamic minimum. *Chem. Soc. Rev.* **2017**, *46* (18), 5536−5550.

(2) Beharry, A. A.; Woolley, G. A. Azobenzene photoswitches for biomolecules. *Chem. Soc. Rev.* **2011**, *40* (8), 4422−37.

(3) Berkovic, G.; Krongauz, V.; Weiss, V. Spiropyrans and Spirooxazines for Memories and Switches. *Chem. Rev.* **2000**, *100* (5), 1741−1754.

(4) Irie, M. Diarylethenes for Memories and Switches. *Chem. Rev.* **2000**, *100* (5), 1685−1716.

(5) Yokoyama, Y. Fulgides for Memories and Switches. *Chem. Rev.* **2000**, *100* (5), 1717−1740.

(6) Filatov, M.; Paolino, M.; Min, S. K.; Kim, K. S. Fulgides as Light-Driven Molecular Rotary Motors: Computational Design of a Prototype Compound. *J. Phys. Chem. Lett.* **2018**, *9* (17), 4995−5001.

(7) Feringa, B. L. In control of motion: from molecular switches to molecular motors. *Acc. Chem. Res.* **2001**, *34* (6), 504−13.

(8) Kienzler, M. A.; Reiner, A.; Trautman, E.; Yoo, S.; Trauner, D.; Isacoff, E. Y. A red-shifted, fast-relaxing azobenzene photoswitch for visible light control of an ionotropic glutamate receptor. *J. Am. Chem. Soc.* **2013**, *135* (47), 17683−6.

(9) Quandt, G.; Hofner, G.; Pabel, J.; Dine, J.; Eder, M.; Wanner, K. T. First photoswitchable neurotransmitter transporter inhibitor: light-induced control of gamma-aminobutyric acid transporter 1 (GAT1) activity in mouse brain. *J. Med. Chem.* **2014**, *57* (15), 6809−21.

(10) Velema, W. A.; Szymanski, W.; Feringa, B. L. Photopharmacology: beyond proof of principle. *J. Am. Chem. Soc.* **2014**, *136* (6), 2178−91.

(11) Garcia-Lopez, V.; Chen, F.; Nilewski, L. G.; Duret, G.; Aliyan, A.; Kolomeisky, A. B.; Robinson, J. T.; Wang, G.; Pal, R.; Tour, J. M. Molecular machines open cell membranes. *Nature* **2017**, *548* (7669), 567−572.

(12) van der Horst, M. A.; Hellingwerf, K. J. Photoreceptor proteins, "star actors of modern times": a review of the functional dynamics in the structure of representative members of six different photoreceptor families. *Acc. Chem. Res.* **2004**, *37* (1), 13−20.

(13) Ernst, O. P.; Lodowski, D. T.; Elstner, M.; Hegemann, P.; Brown, L. S.; Kandori, H. Microbial and animal rhodopsins: structures, functions, and molecular mechanisms. *Chem. Rev.* **2014**, *114* (1), 126−63.

(14) Altun, A.; Yokoyama, S.; Morokuma, K. Quantum mechanical/molecular mechanical studies on spectral tuning mechanisms of visual pigments and other photoactive proteins. *Photochem. Photobiol.* **2008**, *84* (4), 845−54.

(15) Tian, H.; Sakmar, T. P.; Huber, T. The Energetics of Chromophore Binding in the Visual Photoreceptor Rhodopsin. *Biophys. J.* **2017**, *113* (1), 60−72.

(16) Palczewska, G.; Vinberg, F.; Stremplewski, P.; Bircher, M. P.; Salom, D.; Komar, K.; Zhang, J.; Cascella, M.; Wojtkowski, M.; Kefalov, V. J.; Palczewski, K. Human infrared vision is triggered by two-photon chromophore isomerization. *Proc. Natl. Acad. Sci. U. S. A.* **2014**, *111* (50), E5445−54.

(17) Bibikov, S. I.; Grishanin, R. N.; Kaulen, A. D.; Marwan, W.; Oesterhelt, D.; Skulachev, V. P. Bacteriorhodopsin is involved in halobacterial photoreception. *Proc. Natl. Acad. Sci. U. S. A.* **1993**, *90* (20), 9446−50.

(18) Jung, K. H.; Trivedi, V. D.; Spudich, J. L. Demonstration of a sensory rhodopsin in eubacteria. *Mol. Microbiol.* **2003**, *47* (6), 1513−1522.

(19) Kandori, H. Ion-pumping microbial rhodopsins. *Front. Mol. Biosci.* **2015**, *2*, 52.

(20) Nagel, G.; Szellas, T.; Huhn, W.; Kateriya, S.; Adeishvili, N.; Berthold, P.; Ollig, D.; Hegemann, P.; Bamberg, E. Channelrhodopsin-2, a directly light-gated cation-selective membrane channel. *Proc. Natl. Acad. Sci. U. S. A.* **2003**, *100* (24), 13940−13945.

(21) Menon, S. T.; Han, M.; Sakmar, T. P. Rhodopsin: Structural basis of molecular physiology. *Physiol. Rev.* **2001**, *81* (4), 1659−1688.

(22) Nosrati, M.; Berbasova, T.; Vasileiou, C.; Borhan, B.; Geiger, J. H. A Photoisomerizing Rhodopsin Mimic Observed at Atomic Resolution. *J. Am. Chem. Soc.* **2016**, *138* (28), 8802−8808.

(23) Vasileiou, C.; Vaezeslami, S.; Crist, R. M.; Rabago-Smith, M.; Geiger, J. H.; Borhan, B. Protein design: reengineering cellular retinoic acid binding protein II into a rhodopsin protein mimic. *J. Am. Chem. Soc.* **2007**, *129* (19), 6140−6148.

(24) Crist, R. M.; Vasileiou, C.; Rabago-Smith, M.; Geiger, J. H.; Borhan, B. Engineering a rhodopsin protein mimic. *J. Am. Chem. Soc.* **2006**, *128* (14), 4522−4523.

(25) Wang, W. J.; Nossoni, Z.; Berbasova, T.; Watson, C. T.; Yapici, I.; Lee, K. S. S.; Vasileiou, C.; Geiger, J. H.; Borhan, B. Tuning the Electronic Absorption of Protein-Embedded All-trans-Retinal. *Science* **2012**, *338* (6112), 1340−1343.

(26) Ghanbarpour, A.; Nairat, M.; Nosrati, M.; Santos, E. M.; Vasileiou, C.; Dantus, M.; Borhan, B.; Geiger, J. H. Mimicking Microbial Rhodopsin Isomerization in a Single Crystal. *J. Am. Chem. Soc.* **2019**, *141*, 1735−1741.

(27) Gozem, S.; Luk, H. L.; Schapiro, I.; Olivucci, M. Theory and Simulation of the Ultrafast Double-Bond Isomerization of Biological Chromophores. *Chem. Rev.* **2017**, *117* (22), 13502−13565.

(28) Schnedermann, C.; Yang, X.; Liebel, M.; Spillane, K. M.; Lugtenburg, J.; Fernandez, I.; Valentini, A.; Schapiro, I.; Olivucci, M.; Kukura, P.; Mathies, R. A. Evidence for a vibrational phase-dependent isotope effect on the photochemistry of vision. *Nat. Chem.* **2018**, *10* (4), 449−455.

(29) Gueye, M.; Manathunga, M.; Agathangelou, D.; Orozco, Y.; Paolino, M.; Fusi, S.; Haacke, S.; Olivucci, M.; Leonard, J. Engineering the vibrational coherence of vision into a synthetic molecular device. *Nat. Commun.* **2018**, *9* (1), 313.

(30) Agathangelou, D.; Orozco-Gonzalez, Y.; Del Carmen Marin, M.; Roy, P. P.; Brazard, J.; Kandori, H.; Jung, K. H.; Leonard, J.; Buckup, T.; Ferre, N.; Olivucci, M.; Haacke, S. Effect of point

DOI: 10.1021/acs.jpclett.9b00210
J. Phys. Chem. Lett. XXXX, XXX, XXX−XXX

mutations on the ultrafast photo-isomerization of Anabaena sensory rhodopsin. *Faraday Discuss.* **2018**, *207* (0), 55−75.
(31) Mathies, R. A. Photochemistry: A coherent picture of vision. *Nat. Chem.* **2015**, *7* (12), 945−947.
(32) Schapiro, I.; Fusi, S.; Olivucci, M.; Andruniow, T.; Sasidharanpillai, S.; Loppnow, G. R. Initial excited-state dynamics of an N-alkylated indanylidene-pyrroline (NAIP) rhodopsin analog. *J. Phys. Chem. B* **2014**, *118* (42), 12243−12250.
(33) Rossi Paccani, R.; Donati, D.; Fusi, S.; Latterini, L.; Farina, G.; Zanirato, V.; Olivucci, M. Toward a stable alpha-cycloalkyl amino acid with a photoswitchable cationic side chain. *J. Org. Chem.* **2012**, *77* (4), 1738−1748.
(34) Dunkelberger, A. D.; Kieda, R. D.; Shin, J. Y.; Rossi Paccani, R.; Fusi, S.; Olivucci, M.; Crim, F. F. Photoisomerization and relaxation dynamics of a structurally modified biomimetic photoswitch. *J. Phys. Chem. A* **2012**, *116* (14), 3527−3533.
(35) Briand, J.; Bram, O.; Rehault, J.; Leonard, J.; Cannizzo, A.; Chergui, M.; Zanirato, V.; Olivucci, M.; Helbing, J.; Haacke, S. Coherent ultrafast torsional motion and isomerization of a biomimetic dipolar photoswitch. *Phys. Chem. Chem. Phys.* **2010**, *12* (13), 3178−3187.
(36) Leonard, J.; Schapiro, I.; Briand, J.; Fusi, S.; Paccani, R. R.; Olivucci, M.; Haacke, S. Mechanistic origin of the vibrational coherence accompanying the photoreaction of biomimetic molecular switches. *Chem. - Eur. J.* **2012**, *18* (48), 15296−15304.
(37) Roke, D.; Wezenberg, S. J.; Feringa, B. L. Molecular rotary motors: Unidirectional motion around double bonds. *Proc. Natl. Acad. Sci. U. S. A.* **2018**, *115* (38), 9423−9431.
(38) Hall, C. R.; Browne, W. R.; Feringa, B. L.; Meech, S. R. Mapping the Excited-State Potential Energy Surface of a Photomolecular Motor. *Angew. Chem., Int. Ed.* **2018**, *57* (21), 6203−6207.
(39) Haunerland, N. H.; Spener, F. Fatty acid-binding proteins–insights from genetic manipulations. *Prog. Lipid Res.* **2004**, *43* (4), 328−349.
(40) Ragona, L.; Pagano, K.; Tomaselli, S.; Favretto, F.; Ceccon, A.; Zanzoni, S.; D'Onofrio, M.; Assfalg, M.; Molinari, H. The role of dynamics in modulating ligand exchange in intracellular lipid binding proteins. *Biochim. Biophys. Acta, Proteins Proteomics* **2014**, *1844* (7), 1268−1278.
(41) Ragona, L.; Catalano, M.; Luppi, M.; Cicero, D.; Eliseo, T.; Foote, J.; Fogolari, F.; Zetta, L.; Molinari, H. NMR dynamic studies suggest that allosteric activation regulates ligand binding in chicken liver bile acid-binding protein. *J. Biol. Chem.* **2006**, *281* (14), 9697−9709.
(42) Tomaselli, S.; Giovanella, U.; Pagano, K.; Leone, G.; Zanzoni, S.; Assfalg, M.; Meinardi, F.; Molinari, H.; Botta, C.; Ragona, L. Encapsulation of a rhodamine dye within a bile acid binding protein: toward water processable functional bio host-guest materials. *Biomacromolecules* **2013**, *14* (10), 3549−3556.
(43) Pagano, K.; Tomaselli, S.; Zanzoni, S.; Assfalg, M.; Molinari, H.; Ragona, L. Bile acid binding protein: a versatile host of small hydrophobic ligands for applications in the fields of MRI contrast agents and bio-nanomaterials. *Comput. Struct. Biotechnol. J.* **2013**, *6*, No. e201303021.
(44) Tomaselli, S.; Pagano, K.; Boulton, S.; Zanzoni, S.; Melacini, G.; Molinari, H.; Ragona, L. Lipid binding protein response to a bile acid library: a combined NMR and statistical approach. *FEBS J.* **2015**, *282* (21), 4094−4113.
(45) Favretto, F.; Ceccon, A.; Zanzoni, S.; D'Onofrio, M.; Ragona, L.; Molinari, H.; Assfalg, M. The unique ligand binding features of subfamily-II iLBPs with respect to bile salts and related drugs. *Prostaglandins, Leukotrienes Essent. Fatty Acids* **2015**, *95*, 1−10.
(46) Pedo, M.; D'Onofrio, M.; Ferranti, P.; Molinari, H.; Assfalg, M. Towards the elucidation of molecular determinants of cooperativity in the liver bile acid binding protein. *Proteins: Struct., Funct., Genet.* **2009**, *77* (3), 718−731.
(47) Braslavsky, S. E.; Acuna, A. U.; Atvars, T. D. Z.; Bard, A.; Bill, E.; Bjorn, L. O.; Bohne, C.; Bolton, J.; Bonneau, R.; Bouas-Lorent, H.; Braun, A. M.; Dale, R.; Dill, K.; Dopp, D.; Durr, H.; Fox, M.-A.; Gandolfi, T.; Grabowski, Z. R.; Grisbeck, A.; Kutateladze, A.; Litter, M.; Lorimer, J.; Mattay, J.; Michl, J.; Miller, R. J. D.; Moggi, L.; Monti, S.; Nonell, S.; Ogilby, P.; Olbrich, G.; Oliveros, E.; Olivucci, M.; Orellana, G.; Prokorenko, V.; Razi Naqvi, K.; Rettig, V.; Rizzi, A.; Rossi, R. A.; San Roman, E.; Scandola, F.; Schneider, S.; Thulstrup, E. W.; Valeur, B.; Verhoven, J.; Warman, J.; Weiss, R.; Wirz, J.; Zachariasse, K. Glossary of Terms Used in Photochemsitry 3rd Edition (IUPAC Reccomandations 2006). *Pure Appl. Chem.* **2007**, *79* (3), 293−465.
(48) Cogliati, C.; Tomaselli, S.; Assfalg, M.; Pedo, M.; Ferranti, P.; Zetta, L.; Molinari, H.; Ragona, L. Disulfide bridge regulates ligand-binding site selectivity in liver bile acid-binding proteins. *FEBS J.* **2009**, *276* (20), 6011−6023.
(49) Tomaselli, S.; Assfalg, M.; Pagano, K.; Cogliati, C.; Zanzoni, S.; Molinari, H.; Ragona, L. A disulfide bridge allows for site-selective binding in liver bile acid binding protein thereby stabilising the orientation of key amino acid side chains. *Chem. - Eur. J.* **2012**, *18* (10), 2857−2866.
(50) Eliseo, T.; Ragona, L.; Catalano, M.; Assfalg, M.; Paci, M.; Zetta, L.; Molinari, H.; Cicero, D. O. Structural and dynamic determinants of ligand binding in the ternary complex of chicken liver bile acid binding protein with two bile salts revealed by NMR. *Biochemistry* **2007**, *46* (44), 12557−12567.
(51) Lumento, F.; Zanirato, V.; Fusi, S.; Busi, E.; Latterini, L.; Elisei, F.; Sinicropi, A.; Andruniow, T.; Ferre, N.; Basosi, R.; Olivucci, M. Quantum chemical modeling and preparation of a biomimetic photochemical switch. *Angew. Chem., Int. Ed.* **2007**, *46* (3), 414−420.
(52) Karaca, E.; Bonvin, A. M. Advances in integrative modeling of biomolecular complexes. *Methods* **2013**, *59* (3), 372−381.
(53) van Ingen, H.; Bonvin, A. M. Information-driven modeling of large macromolecular assemblies using NMR data. *J. Magn. Reson.* **2014**, *241*, 103−114.
(54) Zheng, M.; Zheng, L.; Zhang, P.; Li, J.; Zhang, Y. Development of bioorthogonal reactions and their applications in bioconjugation. *Molecules* **2015**, *20* (2), 3190−3205.
(55) van Dongen, S. F.; Teeuwen, R. L.; Nallani, M.; van Berkel, S. S.; Cornelissen, J. J.; Nolte, R. J.; van Hest, J. C. Single-step azide introduction in proteins via an aqueous diazo transfer. *Bioconjugate Chem.* **2009**, *20* (1), 20−23.
(56) Cappelli, A.; Grisci, G.; Paolino, M.; Castriconi, F.; Giuliani, G.; Donati, A.; Lamponi, S.; Mendichi, R.; Boccia, A. C.; Samperi, F.; Battiato, S.; Paccagnini, E.; Gentile, M.; Licciardi, M.; Giammona, G.; Vomero, S. Combining spontaneous polymerization and click reactions for the synthesis of polymer brushes: a "grafting onto" approach. *Chem. - Eur. J.* **2013**, *19* (29), 9710−9721.
(57) Lutz, J. F. Nanotechnology for Life Science Research, G. 1,3-dipolar cycloadditions of azides and alkynes: a universal ligation tool in polymer and materials science. *Angew. Chem., Int. Ed.* **2007**, *46* (7), 1018−1025.
(58) Cappelli, A.; Paolino, M.; Grisci, G.; Razzano, V.; Giuliani, G.; Donati, A.; Bonechi, C.; Mendichi, R.; Battiato, S.; Samperi, F.; Scialabba, C.; Giammona, G.; Makovec, F.; Licciardi, M. Hyaluronan-coated polybenzofulvene brushes as biomimetic materials. *Polym. Chem.* **2016**, *7* (42), 6529−6544.
(59) Paolino, M.; Mennuni, L.; Giuliani, G.; Anzini, M.; Lanza, M.; Caselli, G.; Galimberti, C.; Menziani, M. C.; Donati, A.; Cappelli, A. Dendrimeric tetravalent ligands for the serotonin-gated ion channel. *Chem. Commun.* **2014**, *50* (62), 8582−8585.
(60) Lallana, E.; Riguera, R.; Fernandez-Megia, E. Reliable and efficient procedures for the conjugation of biomolecules through Huisgen azide-alkyne cycloadditions. *Angew. Chem., Int. Ed.* **2011**, *50* (38), 8794−8804.
(61) Kumar, A.; Li, K.; Cai, C. Anaerobic conditions to reduce oxidation of proteins and to accelerate the copper-catalyzed "Click" reaction with a water-soluble bis(triazole) ligand. *Chem. Commun.* **2011**, *47* (11), 3186−3188.
(62) Presolski, S. I.; Hong, V. P.; Finn, M. G. Copper-Catalyzed Azide-Alkyne Click Chemistry for Bioconjugation. *Curr. Protoc. Chem. Biol.* **2011**, *3* (4), 153−162.

DOI: 10.1021/acs.jpclett.9b00210
J. Phys. Chem. Lett. XXXX, XXX, XXX−XXX

(63) Ahmad Fuaad, A. A.; Azmi, F.; Skwarczynski, M.; Toth, I. Peptide conjugation via CuAAC 'click' chemistry. *Molecules* **2013**, *18* (11), 13148−13174.
(64) Tomaselli, S.; Ragona, L.; Zetta, L.; Assfalg, M.; Ferranti, P.; Longhi, R.; Bonvin, A. M.; Molinari, H. NMR-based modeling and binding studies of a ternary complex between chicken liver bile acid binding protein and bile acids. *Proteins: Struct., Funct., Genet.* **2007**, *69* (1), 177−191.
(65) Vogeley, L.; Sineshchekov, O. A.; Trivedi, V. D.; Sasaki, J.; Spudich, J. L.; Luecke, H. Anabaena sensory rhodopsin: a photochromic color sensor at 2.0 A. *Science* **2004**, *306* (5700), 1390−1393.
(66) Sineshchekov, O. A.; Trivedi, V. D.; Sasaki, J.; Spudich, J. L. Photochromicity of Anabaena sensory rhodopsin, an atypical microbial receptor with a cis-retinal light-adapted form. *J. Biol. Chem.* **2005**, *280* (15), 14663−14668.
(67) Strambi, A.; Durbeej, B.; Ferre, N.; Olivucci, M. Anabaena sensory rhodopsin is a light-driven unidirectional rotor. *Proc. Natl. Acad. Sci. U. S. A.* **2010**, *107* (50), 21322−21326.
(68) Marin, M. D.; Agathangelou, D.; Orozco-Gonzalez, Y.; Valentini, A.; Kato, Y.; Abe-Yoshizumi, R.; Kandori, H.; Choi, A.; Jung, K. H.; Haacke, S.; Olivucci, M. Fluorescence Enhancement of a Microbial Rhodopsin via Electronic Reprogramming. *J. Am. Chem. Soc.* **2019**, *141* (1), 262−271.

DOI: 10.1021/acs.jpclett.9b00210
J. Phys. Chem. Lett. XXXX, XXX, XXX−XXX